EAAC2025

Microbunching Instability Studies: A Semi-Analytical Insight for EuPRAXIA@SPARC_LAB

Giovanni Campri

Goals and Objectives

- Use a **semi-analytical model** to assess the susceptibility to **Microbunching Instability** (MBI) for specific configurations of EuPRAXIA@SPARC_LAB

- Provide a theoretical outline of a **Laser Heater** (LH) for EuPRAXIA@SPARC_LAB, designed to provide the operational flexibility required to remain **compatible with all the forseen machine configurations**

G. Campri[1,2,3], S. Di Mitri [3,4], A. Giribono [5], C. Vaccarezza [5], M. Ferrario [5]

[1]La Sapienza University of Rome, 00185 Roma, Italy
[2]INFN-Sez. Bologna, 40127 Bologna, Italy
[3]Elettra Sincrotrone Trieste, 34149 Basovizza (TS), Italy
[4]University of Trieste, 34127 Trieste, Italy
[5]Frascati National Laboratories INFN-LNF, 00044 Frascati (RM), Italy

This presentation has received funding from the European Union's Horizon 2020 Research and Innovation programme under GA No 101004730

First user-oriented FEL facility
driven by **plasma wakefield acceleration**
(Currenlty in development)

X-band state of the art technology

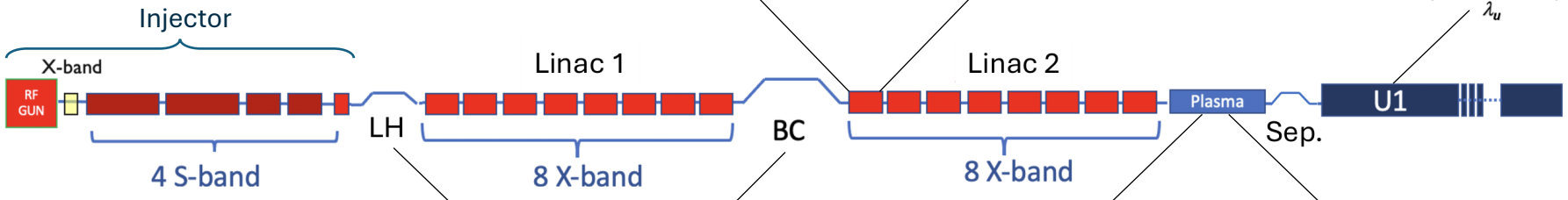

Free-Electron Laser

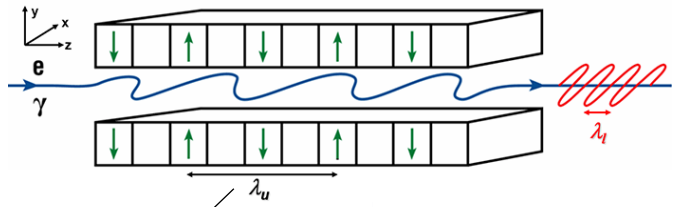

Two magnetic chicanes for **bunch compression**
The first one also hosts the **laser heater**

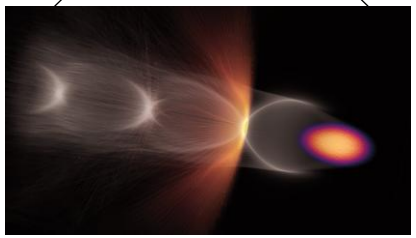

Plasma wakefield acceleration

- Beam energy ~1 GeV
- Driving a SASE FEL
- Ultra-shorts (~fs) high-brilliance pulses
- Operating in the water window spectral region (AQUA beamline)

EuPRAXIA

M. Ferrario, et al. Eupraxia@ sparc_lab design study towards a compact fel facility at Inf. Nuclear Instruments and Methods in Physics Research Section A: Accelerators, Spectrometers, Detectors and Associated Equipment, 909:134–138, 2018.

Microbunching Instability

Initial current inhomogeneities (shot noise)

Energy modulations through impedences (LSC, CSR)

Transformation of energy modulations into amplified **current modulations** through non-isochronous dispersive sections ($R_{56} \neq 0$)

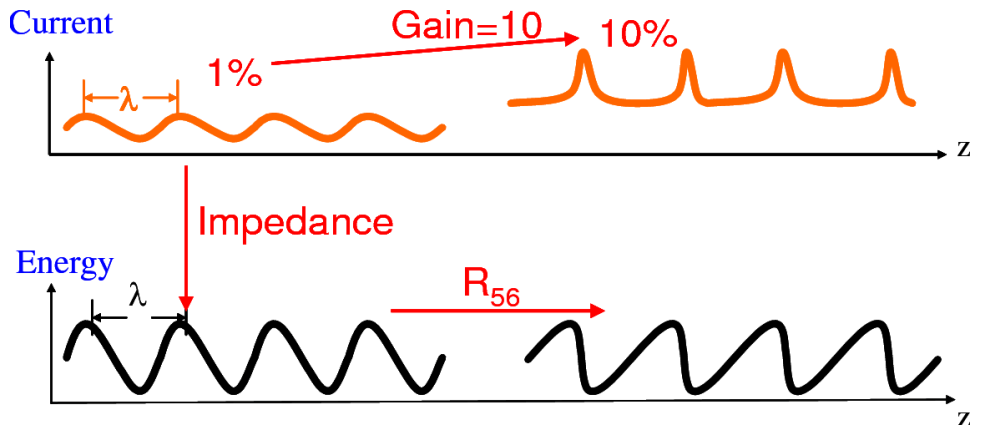

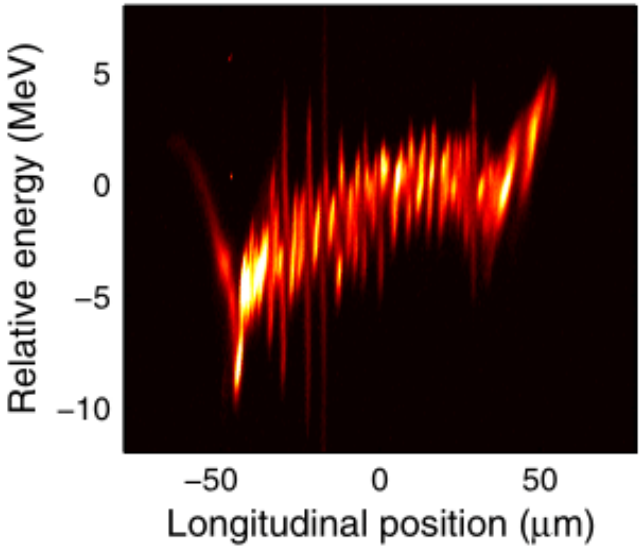

(LCLS)

D. Ratner, et al. Time-resolved imaging of the microbunching instability and energy spread at the linac coherent light source. Physical Review Special Topics-Accelerators and Beams, 18(3):030704, 2015.

Microbunching Instability

Laser heater suppresses the instability through Longitudinal Landau damping

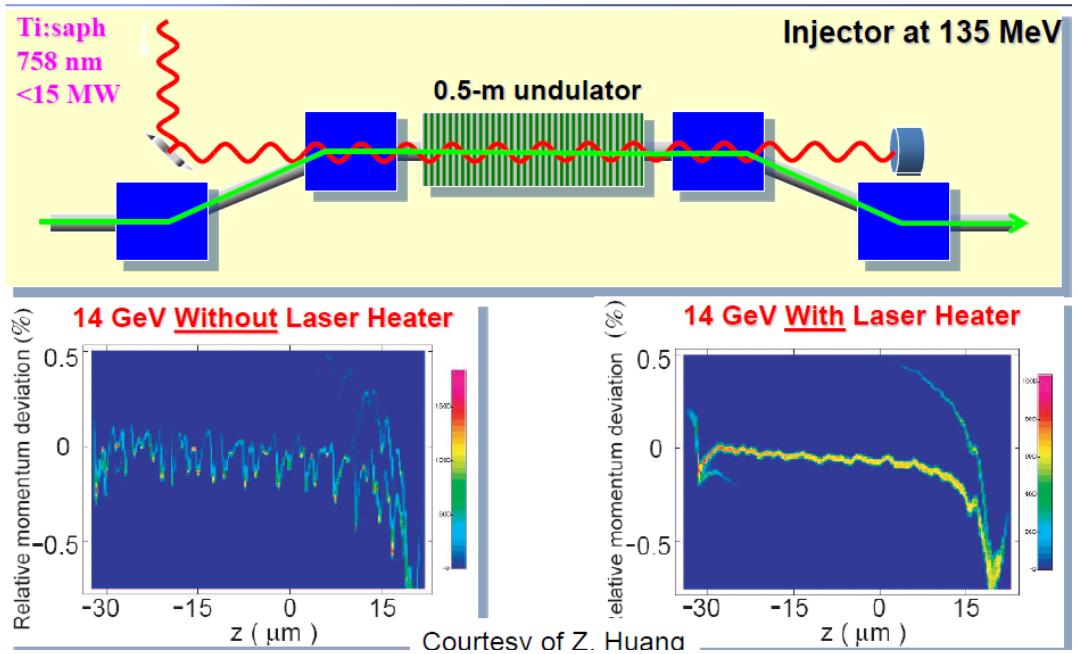

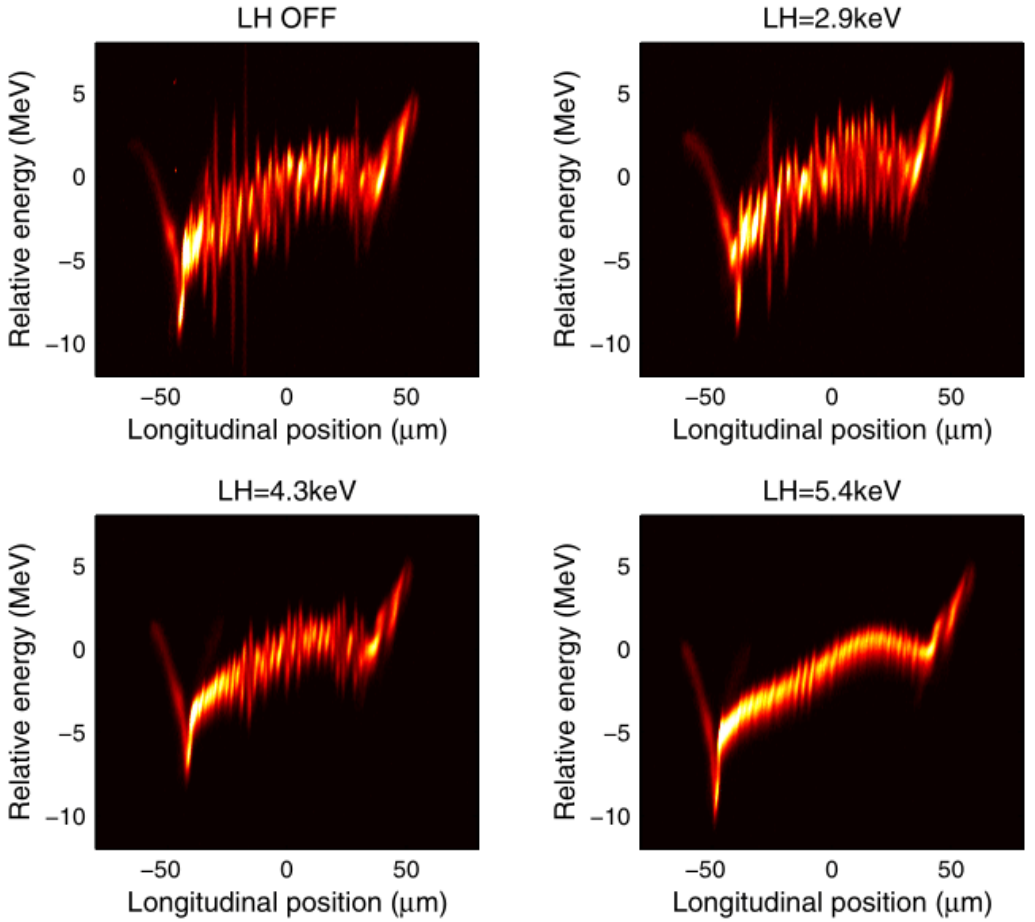

(LCLS)

D. Ratner, et al. Time-resolved imaging of the microbunching instability and energy spread at the linac coherent light source. Physical Review Special Topics-Accelerators and Beams, 18(3):030704, 2015.

Huang-Kim Model

The analytical study of the microbunching instability is carried out in **Fourier space** (the bunching is the Fourier transform of the relative current modulation)

$$b(k) = \frac{1}{\Delta z_b}\int_{-\infty}^{+\infty}\frac{\Delta I(z)}{I_0}e^{-ikz}dz$$

The Huang-Kim formalism is grounded on the linearization of the Vlasov-Maxwell equation for electron beam distribution passing through a **four-dipole symmetric chicane**

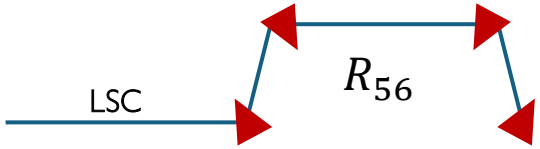

The impedances effects are modeled as an **integral equation** containing the physics of collective effects, including Landau damping

$$b_f(k;s) \approx \frac{CkR_{56}}{\gamma}\overbrace{\frac{4\pi\, I_0}{Z_0 I_A}\int_0^s b_0(k)Z_{LSC}(k;s')ds'}^{\Delta\gamma} LD_{\parallel} \qquad LD_{\parallel} = \exp\left[-\tfrac{1}{2}(CkR_{56}\sigma_\delta)^2\right]$$

The equivalent instability-induced **energy spread** is computed as the integral of the energy modulations over all frequencies

$$\sigma_{MBI} = mc^2\sqrt{2\int_0^\infty \frac{|\Delta\gamma(\lambda)|^2}{\lambda}d\lambda}$$

Z. Huang and K.-J. Kim. Formulas for coherent synchrotron radiation microbunching in a bunch compressor chicane. Physical Review Special Topics- Accelerators and Beams, 5(7):074401, 2002

Huang-Kim Model

Figures of merit to measure the presence of microbunching instability
Evaluated for **witness** and **driver** bunches @**Plasma** and @**Undulator**

Spectral **Gain**

$$G(\lambda) = \left|\frac{b_f}{b_0}\right|$$

Independent of b_0

Relative **energy spread**

$$\sigma_\delta = \frac{1}{E}\sqrt{\sigma_{int}^2 + \sigma_{IBS}^2 + \sigma_{LH}^2 + \sigma_{MBI}^2}$$

Intrisic energy spread (initial ~2 keV) — Intrabeam scattering — Laser heater

Dependent on b_0
(larger cathode laser irregularities will cause a larger energy spread)

Values are to be taken as an indication, since smaller intrinsic energy spread σ_{int} and larger initial bunching b_0 (> shot noise) lead to greater instabilities

Benchmark of measurements @FERMI

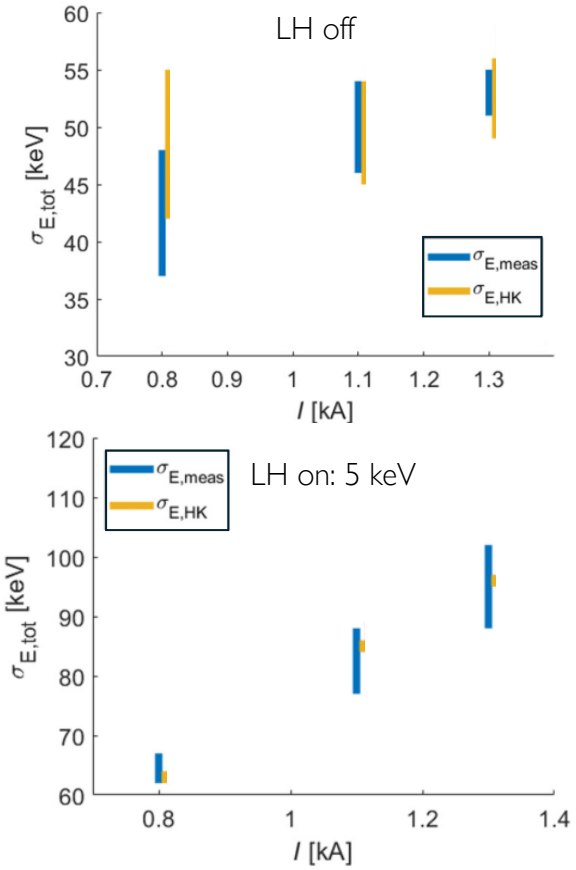

S. Di Mitri, G. Campri, F. Elisii, G. Perosa, and S. Spampinati. Systematic and comprehensive comparison of two semianalytical models of microbunching instability. Physical Review Accelerators and Beams, 28(4):044401, 2025.

EuPRAXIA@SPARC_LAB Configurations

(Contextually to the simulations provided by the SBARC_LAB beam dynamics group)

Three configurations are considered:

COMB beam config.: 400+50 pC

Velocity bunching + Plasma

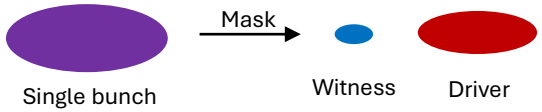

Mask config.: 230+30 pC

Magnetic compression + Plasma

Full-RF config.: 250 pC

Magnetic compression (w/out Plasma)

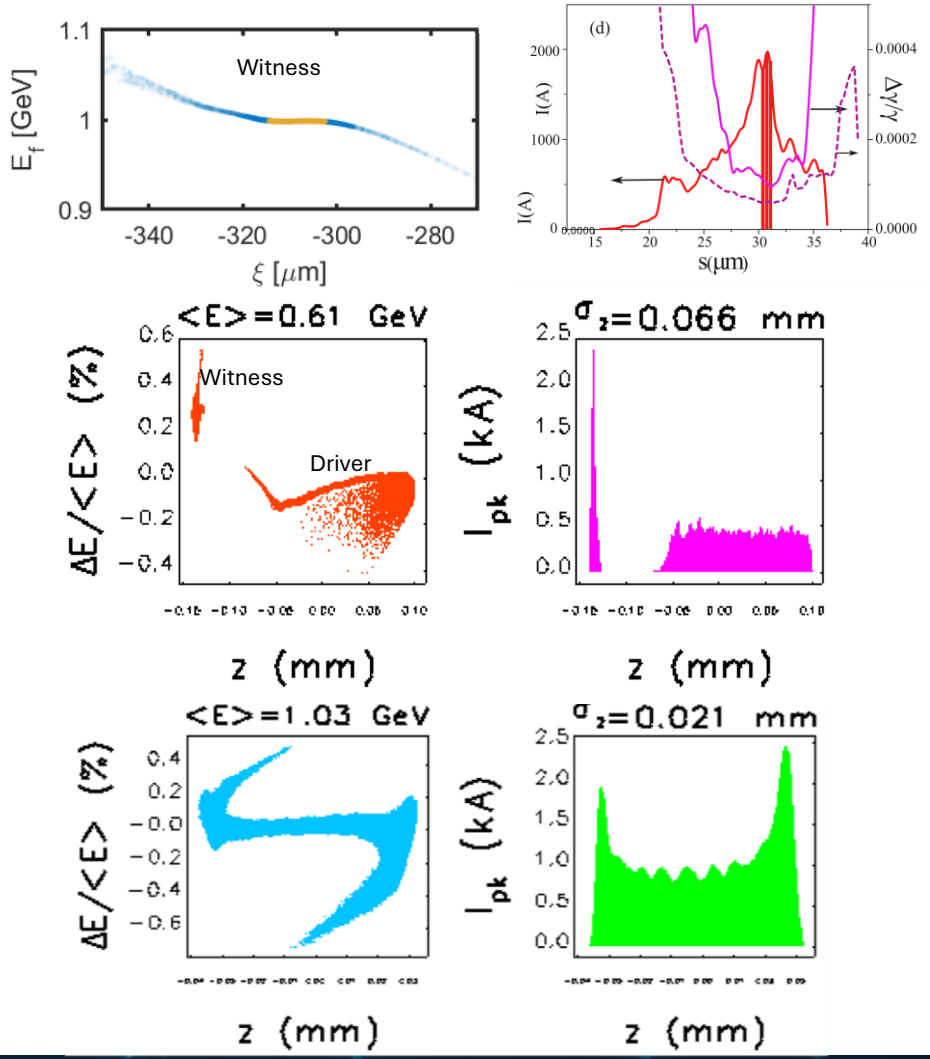

COMB Beam Configuration

COMB beam config.: 400+50 pC

Velocity bunching + Plasma

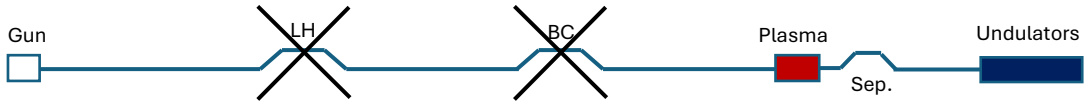

Parameter		COMB	
Beam energy @LH (MeV)		100	
Beam energy @BC (MeV)		330	
Beam energy @Plasma (MeV)		560	
Beam final energy (GeV)		1.0	
LC chicane R_{56}, T_{566}	(mm)	-	
BC chicane R_{56}, T_{566}	(mm)	-	
Sep. chicane R_{56}, T_{566}	(mm)	-1.0, 1.5	
		witness	driver
Q (pC)		50	400
σ_δ @Plasma (‰)		0.1	0.1
σ_δ @Undulator (‰)		0.1	-

$< \rho_{FEL} \sim 10^{-3}$

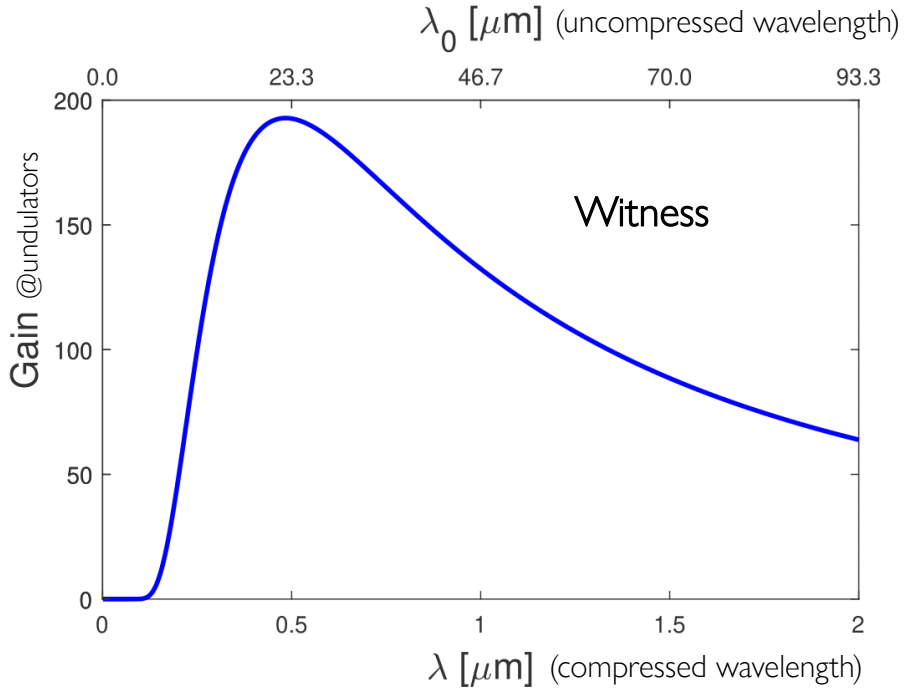

Mask Configuration

Mask config.: 230+30 pC

Magnetic compression + Plasma

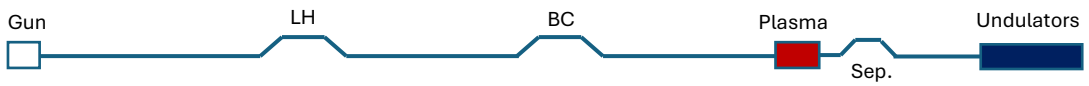

Parameter		Mask
Beam energy @LH (MeV)		270
Beam energy @BC (MeV)		400
Beam energy @Plasma (MeV)		600
Beam final energy (GeV)		1.0
LC chicane R_{56}, T_{566}	(mm)	-60.0, 59.0
BC chicane R_{56}, T_{566}	(mm)	-25.0, 24.0
Sep. chicane R_{56}, T_{566}	(mm)	-1.0, 1.5
	witness	driver
Q (pC)	30	230
σ_δ @Plasma (‰)	0.3	0.1
σ_δ @Undulator (‰)	0.3	-

$< \rho_{FEL} \sim 10^{-3}$

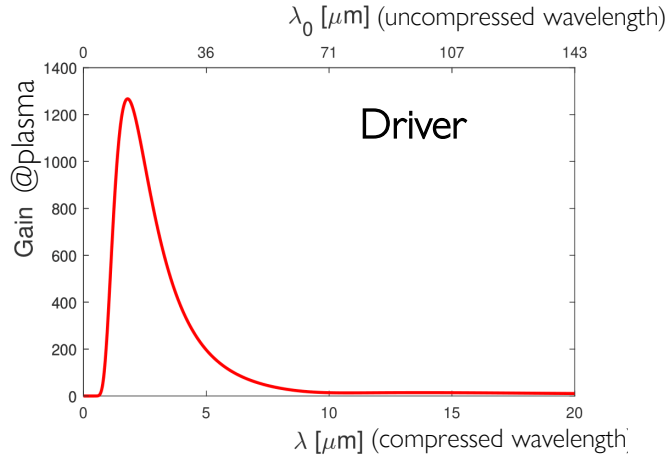

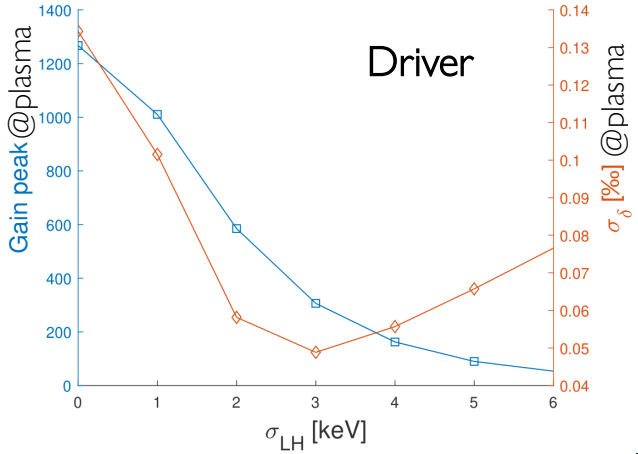

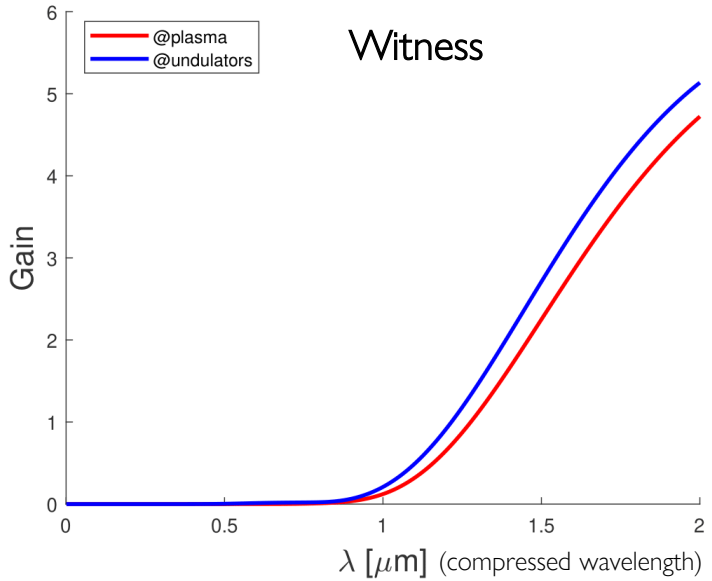

Full-RF Configuration

Full-RF config.: 250 pC

Magnetic compression (w/out Plasma)

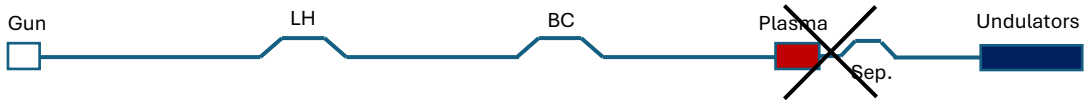

Parameter		Full-RF
Beam energy @LH (MeV)		250
Beam energy @BC (MeV)		670
Beam energy @Plasma (MeV)		-
Beam final energy (GeV)		1.1
LC chicane R_{56}, T_{566}	(mm)	-60.5, 59.7
BC chicane R_{56}, T_{566}	(mm)	-25.0, 24.0
Sep. chicane R_{56}, T_{566}	(mm)	-
		-
Q (pC)		250
σ_δ @Plasma (‰)		-
σ_δ @Undulator (‰)		< 0.1

$< \rho_{FEL} \sim 10^{-3}$

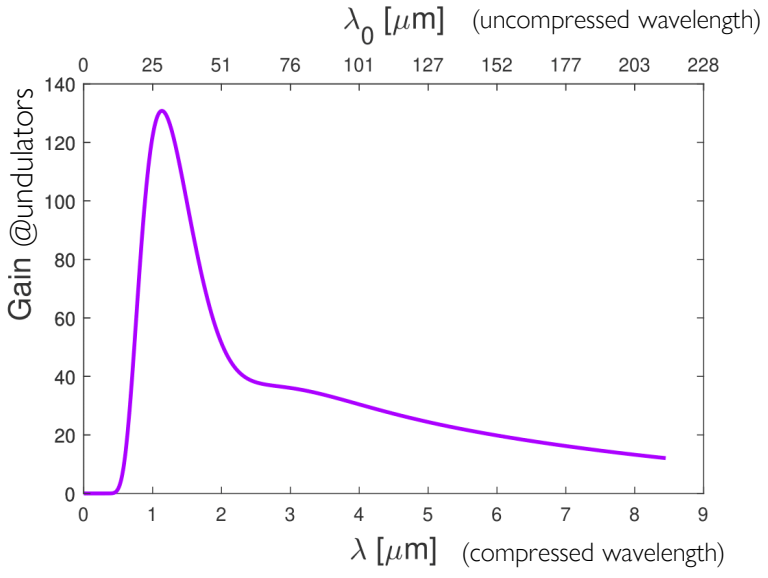

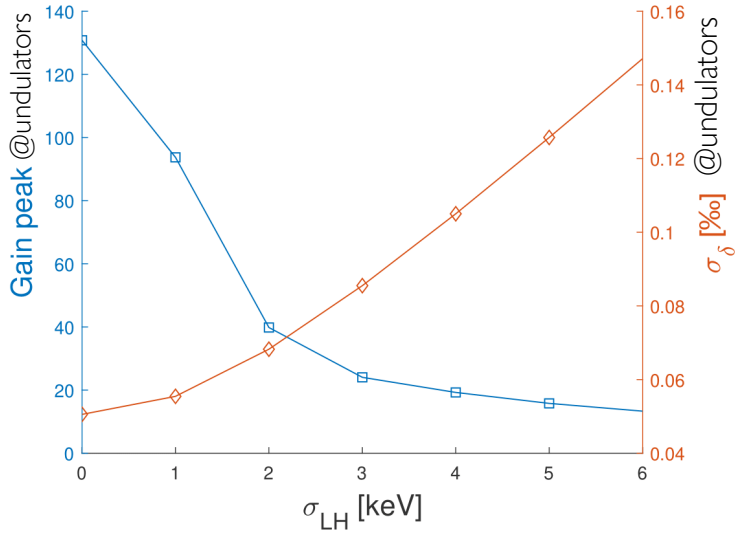

Conclusions

- With the assumed initial beam parameters (initial **shot noise** distribution and **2 keV** intrinsic energy spread) we do not expect major concerns related to the MBI

- **Critical bandwidth** of Gain is expected to be in the range 10-30 μm (uncompressed) for the various configurations tested (linear growth of MBI with b_0)

- The **laser heater** can be used, in case of necessity, to suppress eventual MBI. However, in the case of full compression with velocity bunching, it is not recommended (bunch already compressed, R56 too small for Landau damping, overall inefficient)

Laser Heater Design

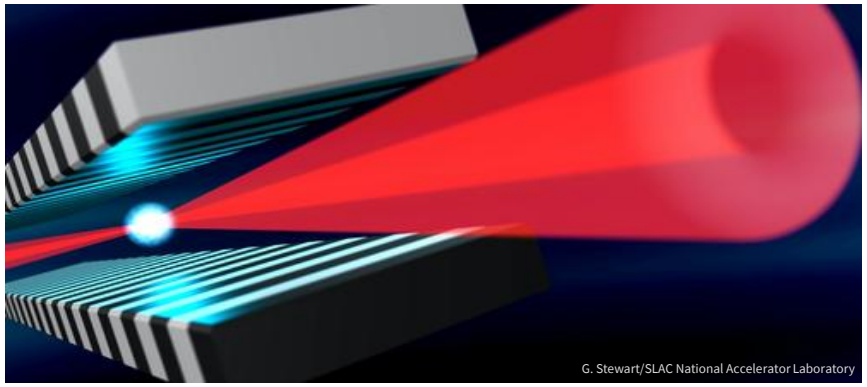

The design of EuPRAXIA@SPARC_LAB **laser heater** system has been studied to accomodate **all possible machine configurations**

The laser heater chicane also have the function of **magnetic bunch compressor**

Variable beam **energy**

100–290 MeV

- Velocity Bunching
- Fully-magnetic Compression

Variable chicane bending **angles**

4–14.5°

- Low Compression
- High Compression

Laser Heater Design

Planar Undulator

- 45 mm period
- 10 periods
- Remanent field 1.2 T
- Full gap 15–35 mm
- Undulator parameter K=0.8–3

Laser System

- Branch of the PIL system (Ti:Sapphire)
- Up to 50 μJ (~5 MW)
- Fundamental harmonic (λ ≈ 800 nm)
- Second harmonic (λ ≈ 400 nm)
- Independent vertical and horizontal focusing

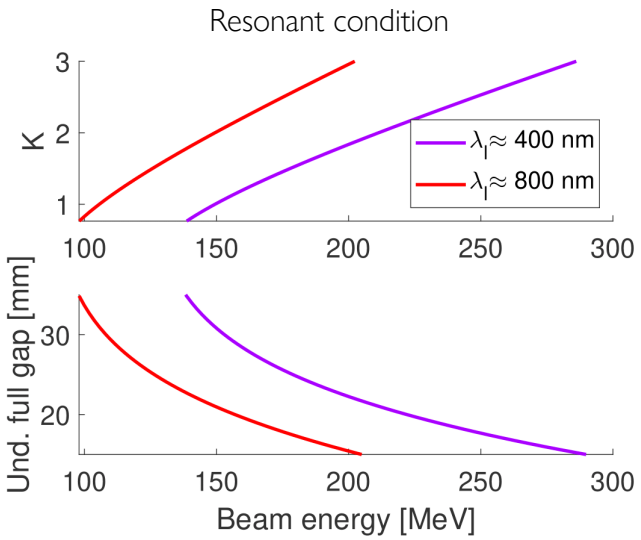

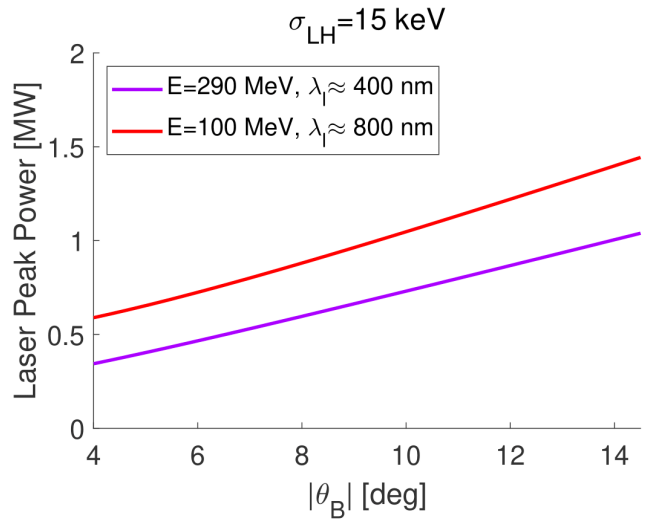

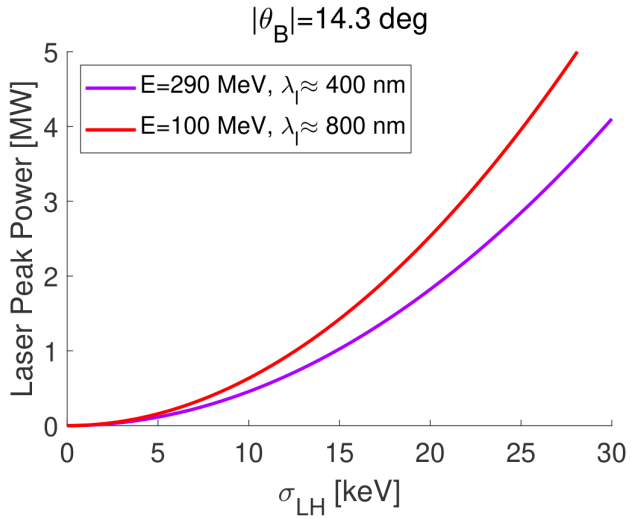

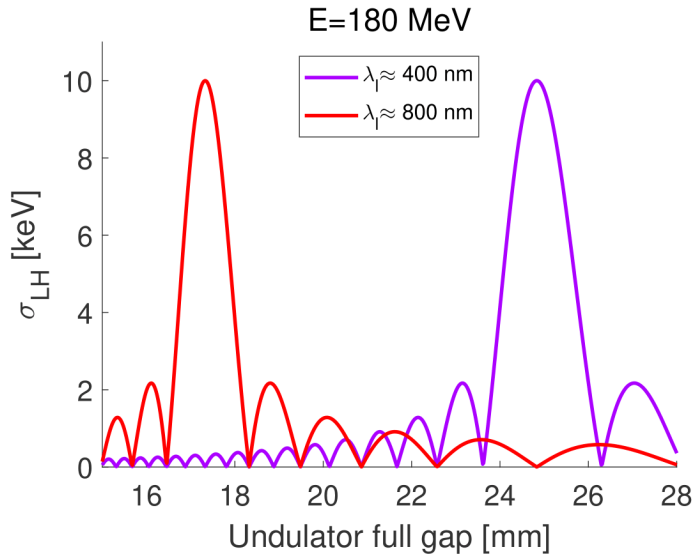

Laser Heater Design

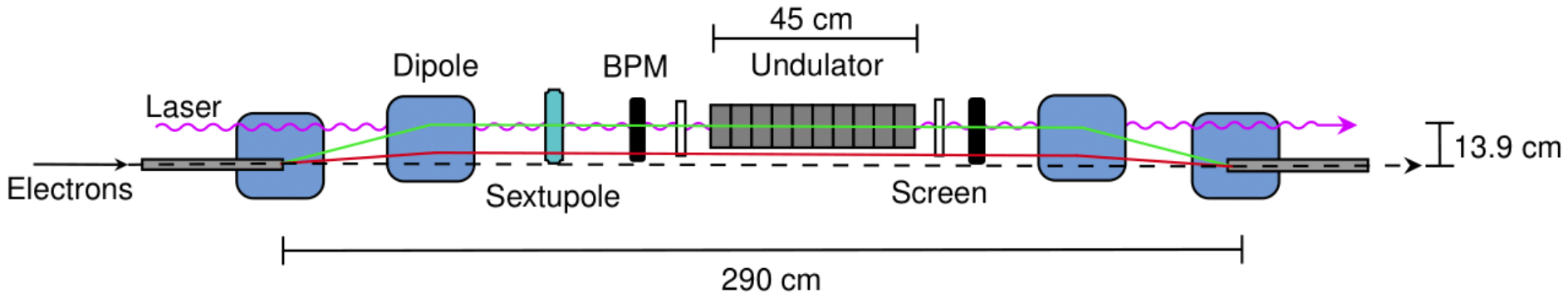

Magnetic Chicane

- Adjustable angles 4–14.5°
- Beam horizontal excursion 39–139 mm
- Common transverse translation stage, movable in a range of ~110 mm

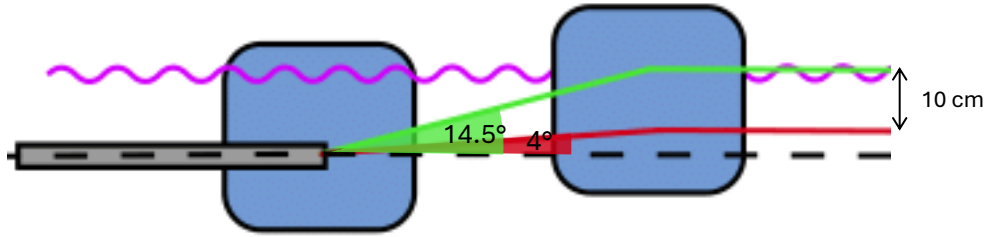

Outlook and Future Developments

- Extensive beam **simulations** complementary to the analytical model

- Study the effects of MBI on the **plasma acceleration** mechanism (current modulations at specific wavelengths)

Thank you for your attention

Longitudinal space charge impedence per unit legth

$$Z_{LSC}(k) = \frac{iZ_0}{k\pi r_b^2}\left[1 - 2I_1\left(\frac{kr_b}{\gamma}\right)K_1\left(\frac{kr_b}{\gamma}\right)\right]$$

Coherent synchrotron radiation impedence per unit length

$$Z_{ICS}(k) = (1.63 + i0.94)\frac{Z_0}{4\pi}\frac{k^{\frac{1}{3}}}{|R|^{\frac{2}{3}}}$$

$Z_0 = 376.73\ \Omega$: Free space impedence

I_1, K_1: Modified Bessel functions

r_b: $0.8735(\sigma_x + \sigma_y)$

IBS-induced energy spread in a single pass linac

$$\sigma_{\delta,IBS}(\gamma;s) = \frac{1}{G_a/(m_e c^2)} \frac{1}{\gamma^2} \int_{\gamma_0}^{\gamma} \tilde{k}(\gamma')\sqrt{\gamma'}\,d\gamma'$$

$$\tilde{k}(\gamma) \approx \left(\frac{N_e r_e}{8\varepsilon_n^{\frac{3}{2}} \beta_\perp^{\frac{1}{2}} \sigma_z} \right) \ln\left(\frac{\beta c \tau N_e \varepsilon_n^{\frac{1}{2}}}{16\gamma^2 \varepsilon_n^{\frac{3}{2}} \beta_\perp^{\frac{1}{2}} \sigma_z} \right)\Bigg|_{\gamma}$$

FERMI end of linac

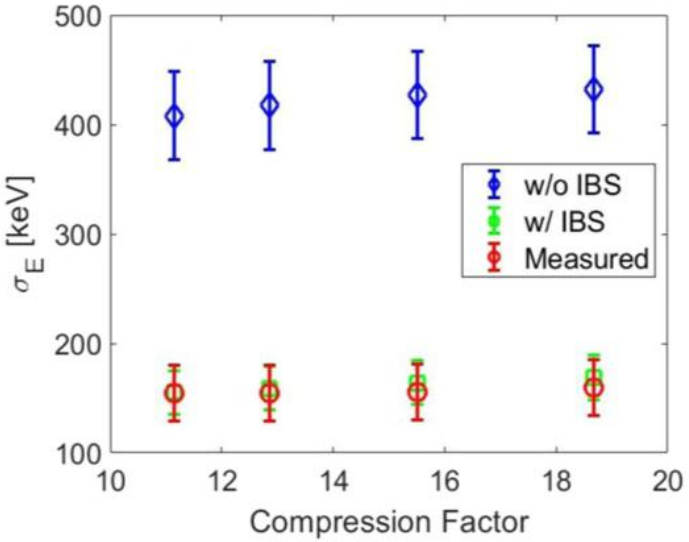

G_a: Average accelerating gradient

N_e: Number of electrons in the bunch

r_e: Classical electron radius

τ: Traveling time

$\beta_\perp$: Average betatron function

S. Di Mitri, G. Perosa, A. Brynes, et al. Experimental evidence of intrabeam scattering in a free-electron laser driver. New Journal of Physics, 22(8):083053, 2020. (and Addendum 2022)